Centrifuge Permeameter for Unsaturated Soils. I: Theoretical Basis and Experimental Developments

Jorge G. Zornberg, M.ASCE[1]; and John S. McCartney, A.M.ASCE[2]

Abstract: A new centrifuge permeameter was developed with the specific objective of expediting the measurement of the hydraulic characteristics of unsaturated soils. The development, theoretical basis, and typical results associated with using the centrifuge permeameter for concurrent determination of the soil-water retention curve (SWRC) and hydraulic conductivity function (K function) of unsaturated soils are presented in this paper. Components developed for the centrifuge permeameter are described, including the centrifuge, permeameter, water flow control system, and instrumentation used to concurrently and nondestructively measure the infiltration rate (flow pump and outflow transducer), volumetric water content (time domain reflectometry), and matric suction (tensiometers) in flight during steady-state infiltration. A companion paper focuses on definition of the SWRC and K function for a clay soil using the procedures described in this paper. While conventional geotechnical centrifuges are used to reproduce the response of earth structure prototypes, the centrifuge developed in this study is used to accelerate flow processes. Accordingly, it required a comparatively small radius (0.7 m) but high angular velocity (up to 875 rpm or 600 g's) to impart a wide range of hydraulic gradients to an unsaturated soil specimen. Analytical solutions to Richards' equation in the centrifuge indicate that steady-state infiltration allows direct determination of the relationships between suction, volumetric water content, and hydraulic conductivity from the instrumentation results. Typical instrumentation results during a drying stage are presented to illustrate determination of data points on the SWRC and K function at steady state. These results were found to be consistent with analytical flow solutions.

CE Database subject headings: Unsaturated soils; Centrifuge; Hydraulic conductivity; Soil water; Experimentation; Theories.

Author keywords: Unsaturated soils; Centrifuge permeameter; Hydraulic conductivity function; Soil water retention curve; TDR; Tensiometers.

Introduction

Many geotechnical systems situated near the ground surface involve unsaturated soils. Yet, traditional analyses of the mechanical and hydraulic response of earth structures generally assume water-saturated conditions. Although this may generally provide a worst-case design scenario, it does not permit optimization of the performance of the system under expected field conditions and thus may lead to overconservative designs. This is particularly relevant in the analysis of geoenvironmental systems, such as evapotranspirative landfill covers, as well as geotechnical systems, such as retaining walls with poorly draining backfill, embankments, and pavement subgrades. Specifically, analyses of water flow in these systems are necessary to determine the spatial and temporal variations in pore-water pressure and seepage rates. The cornerstones of water flow analyses are the hydraulic char-

acteristics of the unsaturated soils. This includes the soil-water retention curve (SWRC) and the hydraulic conductivity function (K function), a set of relationships that govern their moisture storage and impedance to water flow, respectively (Fredlund and Rahardjo 1995; Lu and Likos 2005). One of the challenges of analyses involving unsaturated conditions is that measurement of the hydraulic characteristics of unsaturated soils involves lengthy testing time requirements. Consequently, most projects requiring the use of hydraulic characteristics of unsaturated soils rely heavily on empirical correlations or theoretical models rather than on experimental measurement of the hydraulic characteristics.

Flow of water in unsaturated soils can be described using three nonlinearly related variables, namely, the volumetric water content θ (or degree of saturation), the matric suction ψ (or capillary pressure if the air pressure is nonzero), and the hydraulic conductivity K. The SWRC is defined as the relationship between θ and ψ and represents the energy needed (i.e., ψ) to desaturate the soil to a given θ. The K function is defined as the relationship between K and ψ (or θ) and reflects the decrease in available pathways for water flow as a soil desaturates.

The typical SWRC and K function of a clay with low plasticity are shown in Fig. 1. The experimental SWRC data shown in this figure were obtained using three of the four approaches described by ASTM D6836 (ASTM 2002) (i.e., the hanging column test, pressure chamber test with volumetric outflow measurements, and chilled mirror hygrometer test). It is important to note that each point on the SWRC in Fig. 1 was defined using a different water flow mechanism. The hanging column and pressure chamber tests involve monitoring the transient outflow of water from the soil

[1]Fluor Centennial Associate Professor, Geotechnical Group, Dept. of Civil Engineering, The Univ. of Texas at Austin, 1 Univ. Station, C1792, Austin, TX 78712-0280. E-mail: zornberg@mail.utexas.edu

[2]Barry Faculty Fellow and Assistant Professor, Dept. of Civil, Environmental, and Architectural Engineering, Univ. of Colorado at Boulder, UCB 428, Boulder, CO 80309 (corresponding author). E-mail: john.mccartney@colorado.edu
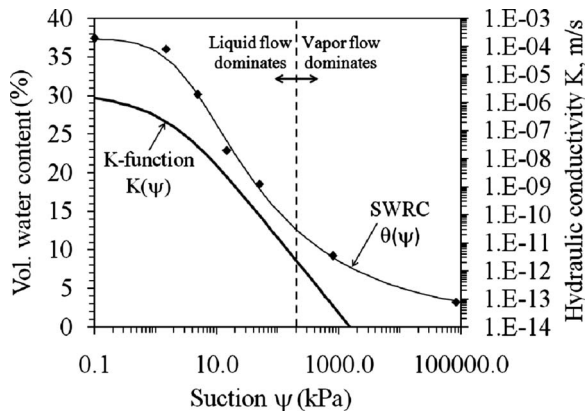
Fig. 1. Hydraulic characteristics of an unsaturated clay of low plasticity

specimen during application of a matric suction ψ (i.e., the difference between the pore air and pore-water pressure), while the hygrometer test involves monitoring the total suction (i.e., the sum of matric and osmotic suction values) during evaporation of water from the soil. Instead of using experimentally derived data as in the SWRC, the K function shown in Fig. 1 was defined using a theoretical model. Specifically, the van Genuchten–Mualem (van Genuchten 1980) model was used to define the K function of the soil. This assumes that the soil behaves as a bundle of capillary tubes having properties described by the parameters of a function fitted to the experimental SWRC data of the soil. The predicted K function in Fig. 1 is only shown up to a K of 10^{-14} m/s as this value is near the low end of K values that have been measured for soils in the laboratory (Olson and Daniel 1981). The K function represents the proportionality between the hydraulic gradient and water flow rate and is thus only relevant for conditions in which the water phase in the soil is continuous. When the water phase in the soil becomes discontinuous, hydraulic gradients applied to the water phase will not result in water flow. Instead, vapor transport by diffusion dominates the migration of water in the soil. Because the theoretical prediction of the K function provides no lower bound on the K of a soil, the boundary between liquid and vapor phase transport is difficult to assess. This boundary is likely to occur in the vicinity of the ψ value where the slope of the SWRC starts to decrease or at about 200 kPa for the data in Fig. 1.

The common practice of predicting the shape of the SWRC and K function using empirical observations or theoretical models is well documented [e.g., Zapata et al. (1999), van Genuchten (1980), and Brooks and Corey (1964)]. Nonetheless, experimental evaluations of the validity of predicted K functions are rarely conducted in practice. This is especially problematic as the SWRC and K function are sensitive to soil structure variables such as pore size distribution (Arya et al. 1999; Burger and Shackelford 2001; Simms and Yanful 2002; Chiu and Shackelford 1998), flocculated or dispersed soil structures (Vanapalli et al. 1999), mineralogy (Miller et al. 2002), compaction conditions (Meerdink et al. 1996; Tinjum et al. 1997), use of admixtures (Puppala et al. 2006), volume changes (Huang et al. 1998; Parent et al. 2007), and stress state (Ng and Pang 2000). The hydraulic characteristics can show hysteretic behavior upon wetting and drying (Topp and Miller 1966), so they are not unique soil properties as often considered in empirical and theoretical predictions. Khaleel et al. (1995) observed that predicted K functions could be in error by several orders of magnitude due to some of these

effects. The range of variables that affect the k function and the high magnitude of errors associated with prediction add emphasis to the need for experimental measurement of the hydraulic characteristics of unsaturated soils.

The only test available so far to directly measure the hydraulic characteristics using controlled infiltration governed by Darcy's law is the column flow test performed in either a rigid-wall permeameter with flow controlled by surface infiltration and gravity drainage or in a flexible-wall triaxial permeameter with flow controlled by a pump. Specifically, a column flow test can be used to measure the SWRC and K function by imposing a known rate of water flow through the specimen and monitoring the corresponding gradient in hydraulic head or by imposing a gradient in hydraulic head on the specimen and monitoring the ensuing flow rate. In either approach, there will be a transient period during which θ and ψ will change, followed by a period during which water flow will occur under steady-state conditions. Although the transient changes in θ and ψ can be used to measure the soil hydraulic characteristics (Olson and Daniel 1981), the calculated flow rates and gradients are prone to significant scatter. Although steady-state flow data can also be used to measure the hydraulic characteristics with more confidence, a significantly long time is needed to establish different steady flow conditions (Moore 1939; McCartney et al. 2007).

This study focuses on the concurrent experimental measurement of both the SWRC and K function using a new centrifuge permeameter that addresses the shortcomings of previous approaches. Specifically, a new centrifuge permeameter was developed and implemented at the Univ. of Texas (UT) at Austin to allow generation of reliable information that can be obtained under steady-state conditions in instrumented column flow tests. Although similar in concept, the new centrifuge permeameter requires much shorter testing time than column flow tests. Centrifuge technology has been used in previous studies as a means of decreasing testing time when using steady-state infiltration for characterization of unsaturated soils. This was the motivation behind the development of the steady-state centrifuge (SSC) by Nimmo et al. (1987) and of the unsaturated flow apparatus (UFA) by Conca and Wright (1992), which has been standardized as test method ASTM D6527 (ASTM 2000). The UFA approach has been employed in geotechnical design for measurement of the hydraulic characteristics of soil used in alternative landfill covers (Zornberg et al. 2003). However, the SSC and UFA use relatively small medical ultracentrifuges, which do not include a data acquisition system that is operational under high centripetal accelerations. Consequently, these systems do not permit concurrent measurement of the SWRC and K function of soils. Additional shortcomings include the lack of instrumentation for in-flight verification of the theoretical basis behind the interpretation of results as well as the use of comparatively small soil specimens. Despite these shortcomings, the SSC and UFA methods can be practical tests if their underlying assumptions are validated with a more complete test method such as that presented herein.

This study presents details of the centrifuge developed at UT at Austin, including the permeameter, water flow control systems, details and calibration of instrumentation, the theoretical basis for data reduction to measure the SWRC and K function of a soil, and typical experimental results to define a data point on the SWRC and K function. A companion paper (McCartney and Zornberg 2010) presents the analysis of results from infiltration tests performed in the centrifuge permeameter with the objective of determining, using a single soil specimen, the full set of hydraulic
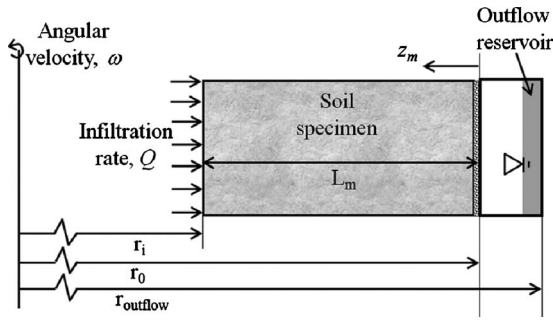
Fig. 2. Schematic view of a centrifuge permeameter with relevant variables

characteristics of a low plasticity clay along both drying and wetting paths.

Background on Water Flow in a Centrifuge Permeameter

Centrifuges are used in many industrial applications to separate liquids from solids. In the particular case of a centrifuge permeameter, centrifugation leads to an increased acceleration field, which in turn results in an increased hydraulic gradient across the soil specimen. The centripetal acceleration, oriented outward in a radial direction and at a distance r from the axis of rotation, equals

$$a = \omega^2 r = N_r g \qquad (1)$$

where ω = angular velocity of the centrifuge; g = acceleration due to gravity; and N_r = ratio between the centripetal acceleration and g. The subscript r in N_r signifies that N varies (linearly) with the radius.

A schematic view of the centrifuge permeameter is shown in Fig. 2. The permeameter contains a cylindrical soil specimen with length L_m and diameter of D that spins in a centrifuge around a central axis at an angular velocity ω. Consistent with the notation used by Dell'Avanzi et al. (2004), the subscript m is used in variables associated with the centrifuge model that can be scaled to a geometrically equivalent prototype soil layer. The permeameter has an inlet face at a radius r_i and an outlet face at a radius r_0. To be consistent with the convention used in 1-g column tests, a coordinate z_m is defined as positive from the base of the specimen toward the central axis of rotation (Dell'Avanzi et al. 2004) as follows:

$$z_m = r_0 - r \qquad (2)$$

The value of N_r at midheight ($z_m = L_m/2$) of the specimen $N_{r,mid}$ is referred in this study as the "g level" and is used to provide a single representative value of N_r. This does not imply that the g level is constant through the specimen.

As in the case of water flow under normal gravity, water flow under a centrifugal field is driven by a gradient in total hydraulic head. The components of the total hydraulic head are the water pressure head, the osmotic pressure head, the potential (or elevation) head, and the water velocity head. The magnitudes of steady-state seepage velocities imposed in this study are less than 10^{-4} m/s, so the velocity head component is negligible. The osmotic pressure does not vary with θ in soils except under nearly dry conditions (Villar 2002), so its gradient is negligible and can be ignored in water flow analyses. Additional discussion on these

components is provided by McCartney (2007). The centrifuge permeameter described in this study was intended to permit free movement of air into and out of the soil specimen, so the pore air pressure P_a is assumed to be atmospheric (i.e., $P_a = 0$). Accordingly, ψ can be substituted for the water pressure P_w (i.e., $\psi = -P_w$). Considering these assumptions, the hydraulic head in the centrifuge h_m is given by

$$h_m = -\frac{\omega^2}{2g}(r_0 - z_m)^2 - \frac{\psi}{\rho_w g} \qquad (3)$$

The first and second terms on the right-hand side of Eq. (3) correspond to the centrifuge elevation head and the suction head, respectively. Consistent with Darcy's law, $K(\psi)$ is the coefficient of proportionality between the water discharge velocity through the soil specimen v_m and the gradient in total hydraulic head h_m along the length of the specimen. Nimmo et al. (1987) reported that the flow of water through soils in the centrifuge follows Darcy's law for g levels below 1,600 g's. As z_m is defined as positive toward the axis of rotation, v_m is positive in the direction of increasing z_m (toward the axis of rotation). The derivative with respect to z_m of the total hydraulic head (i.e., dh_m/dz_m) can be obtained from Eq. (3) and incorporated into Darcy's law to define the discharge velocity v_m as follows:

$$v_m = -K(\psi)\left[\frac{\omega^2}{g}(r_0 - z_m) - \frac{1}{\rho_w g}\frac{\partial \psi}{\partial z_m}\right] \qquad (4)$$

As will be shown later in this paper for conditions representative of the centrifuge permeameter, the first term within the brackets (the gradient in centrifuge elevation head) is generally much greater than the second term (the gradient in suction head). During steady-state water flow, the imposed discharge velocity v_m remains constant with respect to both time and elevation z_m. Accordingly, as z_m is present on the right hand side of Eq. (4), the K must also vary along the soil specimen during centrifuge testing. This should be accounted for in the interpretation of results from the centrifuge permeameter, as will be discussed in Section 6 of this paper.

Early centrifuge permeameter studies (Briggs and McLane 1907; Gardner 1937) did not involve steady flow through a soil specimen. In these centrifuges, water was permitted to drain from an initially saturated specimen while imposing a known suction $\psi(0)$ at $z_m = 0$. After outflow stops ($v_m = 0$), the specimen was said to be at equilibrium. In this case, the ψ profile in the soil specimen can be obtained by integrating ψ from Eq. (4) as follows:

$$\psi(z_m) = \frac{\rho_w \omega^2}{2}[2r_0 z_m - z_m^2] + \psi(0) \qquad (5)$$

The SSC and UFA approaches use a simplified form of Eq. (4) in which the ψ gradient is neglected. This assumption allows definition of K as a function of gravimetric water content, which is obtained by stopping the centrifuge periodically and measuring the changes in weight of the soil specimen until steady-state conditions are observed. Results from separate tests, conducted under no influx, are interpreted using Eq. (5) to define the SWRC. In contrast, the results obtained with the centrifuge permeameter developed in this study allow direct simultaneous measurement of both the SWRC and K function without adopting simplifications to Eq. (4).
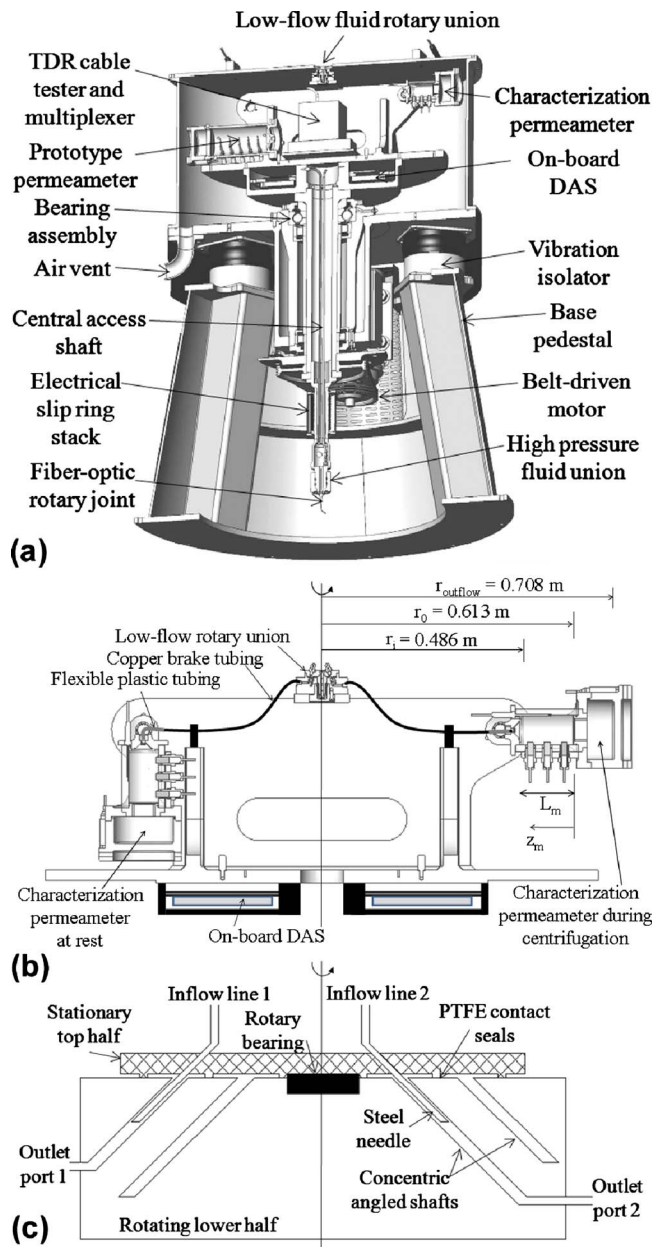
Fig. 3. Centrifuge permeameter setup: (a) centrifuge; (b) testing environment and data acquisition hub; and (c) low-flow rotary union

Centrifuge Permeameter System

The centrifuge at the UT at Austin, developed as part of this study, was constructed by Thomas Broadbent and Sons, LLC of Huddersfield, U.K. A cross section of the centrifuge is shown in Fig. 3(a). The centrifuge includes a testing environment and data acquisition hub resting atop a spindle and bearing assembly, which is supported by three vibration isolators mounted on a conical base pedestal. A central access shaft in the spindle permits wires and plumbing lines to pass through rotary joints (e.g., an electrical slip ring stack, a high pressure fluid union, and a fiber-optic rotary joint) from the data acquisition system and testing environment to the stationary environment. A belt-driven electric motor is used to spin the centrifuge. For illustrative purposes, two permeameter types are shown in the testing environment in Fig. 3(a), although only one type can be used at a time. The charac-

terization permeameter, which is the focus of this paper, is shown on the right side of the environment, while a prototype permeameter used to model water flow through layered soil profiles is shown on the left side (Nimmo 1990).

The testing environment is shown with added detail in Fig. 3(b). Two identical instrumented characterization permeameters are integral components of a swinging bucket assembly. The swinging buckets, mounted diametrically opposite to each other on a steel support frame, permit the longitudinal axis of the permeameter to be aligned with the resultant of the acceleration field. Characterization permeameters at rest (left) and spinning (right) are shown in Fig. 3(b) along with distances from the central axis of the centrifuge to different locations in the testing environment during centrifugation.

In the SSC centrifuge proposed by Nimmo et al. (1987), the infiltration rate was controlled by a system of reservoirs and saturated porous stones that applied a constant infiltration rate to a soil specimen. Disadvantages of this system are that the infiltration rate cannot be controlled independently of the angular velocity and that the porous stones must be changed to apply different infiltration rates. Instead, the centrifuge permeameter used in this study used a two-channel infusion pump outside of the centrifuge to supply a constant infiltration rate, independent of the angular velocity, to a two-channel low-flow rotary union connected to the permeameter. A similar approach was implemented in the UFA centrifuge (Conca and Wright 1992). The infusion pump was selected as it can apply large volumes of liquid using continuous steady flow rates ranging from 0.1 to 1,000.0 mL/h. Syringe pumps driven by a screw drive can also be used with the centrifuge if lower discharge velocities are needed. Distilled water was used in the infiltration tests performed as part of this study, although the infusion pump allows use of any fluid (tap water, natural pore fluid, leachate, and nonaqueous-phase liquids).

The low-flow rotary union, shown in Fig. 3(c), was designed to transmit low-flow rates while preventing water loss and minimizing heat generation. Also, this system allowed operation without water pressurization, which was necessary as air was intended to move freely through the specimen during testing, similar to large-scale column flow tests. The rotary union consists of upper and lower disks. The lower rotating disk is made of steel and includes two inclined concentric channels. These channels are plumbed to exit ports on opposite sides of the rotary union from where water flows into the diametrically opposite permeameters. The upper stationary disk is made from polytetrafluoroethylene (PTFE), which provides a low-friction interface contact with the steel lower disk while preventing water leakage from the rotating interface. To ensure nominal contact between the upper and lower disks, the upper PTFE disk is suspended on a bearing assembly. The PTFE disk also includes two steel needles placed at the same radial locations and inclinations as the inclined channels in the lower chamber. Fluid from the infusion pump drips from the steel needles of the upper disks into the concentric channels of the lower disk. The fluid moves toward the outside radius of the inclined channels during centrifugation and drain through the exit ports on the sides of the lower disk. Copper brake tubing, which remains rigid during centrifugation but can still be bent into desired shapes, is used to transmit water from the rotary union to the characterization permeameters.

The centrifuge developed as a part of this study has a maximum angular velocity of 875 rpm, which translates to a g level of 600 at the base of the outflow reservoir ($r_0 = 0.71$ m). The swinging buckets of the characterization permeameter have a maximum payload of 50 kg (including a maximum of 10 kg of soil) for a
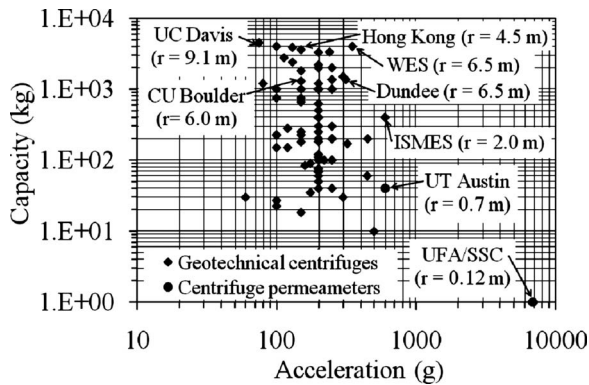
Fig. 4. Comparison of the capacity rating and maximum angular velocity for the centrifuge permeameter with those for medical and geotechnical centrifuges

g-ton rating of 30. The maximum capacity and speed of the centrifuge are shown in Fig. 4 along with those of other geotechnical centrifuges [International Society for Soil Mechanics and Foundation Engineering (ISSMGE) 1998] and the medical centrifuges used by the UFA and SSC (Nimmo et al. 1987; Conca and Wright 1992). Geotechnical centrifuges are typically tailored to address the mechanical response of earth structures rather than to investigate flow phenomena, so a higher payload and radius are desirable. The only centrifuges that can impose a higher acceleration than the centrifuge permeameter developed in this study are the medical centrifuges used by the UFA and SSC, although the capacity (0.5 kg) and radius (0.12 m) of these centrifuges are much smaller, preventing the use of an in-flight data acquisition system.

The main components of the characterization permeameter are shown in the isometric schematic in Fig. 5(a). The permeameter basket is supported on a pivot arm using low-friction rotary bearings. An outflow reservoir with a capacity of 1 L is attached to the base of the permeameter basket and can be removed for use in the characterization or prototype permeameters. The characterization permeameter is held within the permeameter basket and can be removed for preparation of soil specimens outside of the centrifuge. A soil specimen inside the permeameter is supported by a platen that is integrated into the bottom of the permeameter basket and is plumbed to permit free exit of water from the specimen directly into the outflow reservoir. The fluid distribution cap, which is used to distribute water uniformly to the upper surface of the specimen, fits within the top of the permeameter and is attached to the permeameter basket with a pair of screws.

The characterization permeameter, a cross section of which is shown in Fig. 5(b), is an acrylic cylinder with an inside diameter of 71 mm (2.8 in.), a wall thickness of 25 mm, and a specimen height of 127 mm (5.0 in.). The inside diameter is slightly less than a typical 76.2-mm diameter Shelby tube, which permits an undisturbed specimen to be trimmed into the permeameter. The length of the permeameter was selected to provide ample clearance for instrumentation. Acrylic was selected for the permeameter due to its transparency and low electrical conductivity. The permeameter has a collar with a height of 15.2 mm which can be removed to allow trimming of compacted specimens to the desired height. After trimming, the collar is replaced on the permeameter and is used to support the fluid distribution cap, as shown in Fig. 5(b).

The fluid distribution cap is intended to apply an infiltration rate uniformly to the upper surface of the soil specimen without restricting movement of air. Water passes through the copper

(a)

(b)

(c)
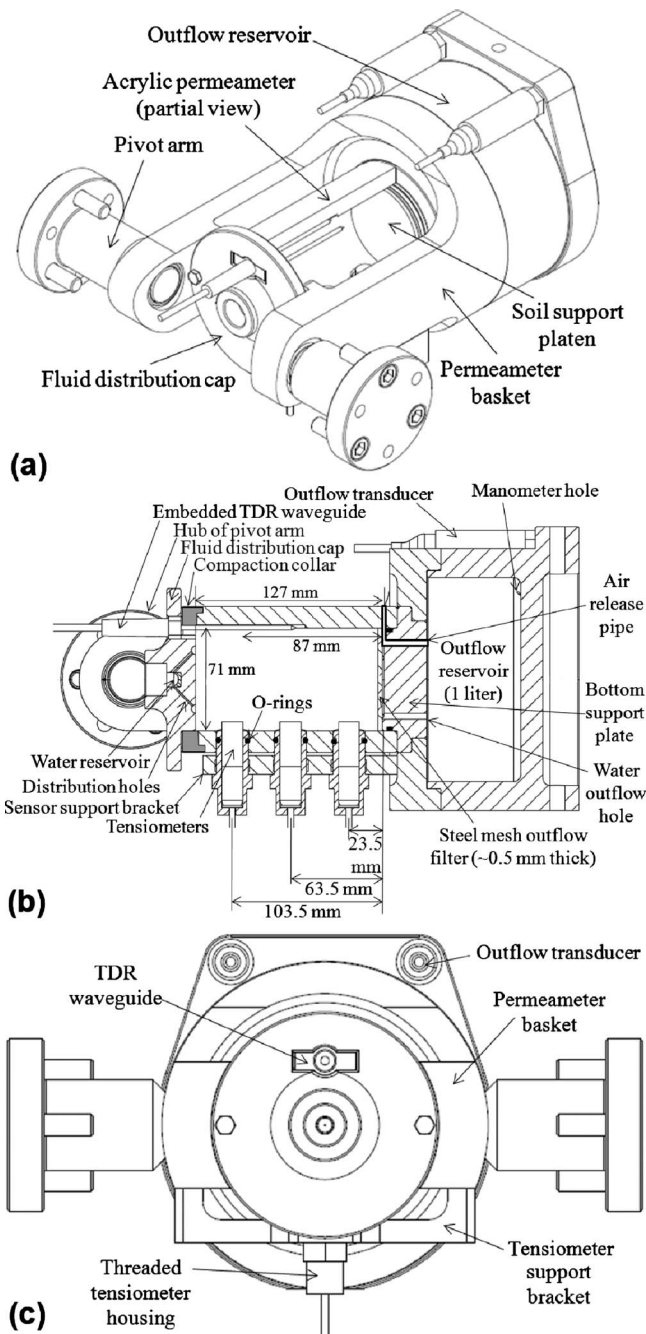
Fig. 5. Schematics of the hydraulic characterization permeameter: (a) isometric view; (b) cross-sectional view with instrumentation locations; and (c) plan view

brake tubing from the rotary joint and drips into a hemispherical reservoir in the top of the fluid distribution cap. This is shown in Fig. 5(b) as well as in the plan view of the permeameter setup in Fig. 5(c). Water accumulates in this reservoir until reaching the level of eight distribution holes, as shown in Fig. 5(b). These 1.6-mm-diameter distribution holes lead to equally spaced locations on the surface of the specimen. Tests conducted to capture the outflow from each of the overflow holes confirmed that the inflow was evenly distributed among the holes. In addition, several filter papers were placed between the soil and fluid distribution cap, with 1.0-mm holes punched in the paper for air escape. The overflow holes and filter papers facilitated uniform distribution of water flow across the upper surface of the soil specimen.

The fluid distribution cap is sheltered within the arms of the permeameter, which minimize the effects of windage on the top of the permeameter. Accordingly, the air pressure can assumed to be equal to atmospheric conditions.

The bottom (outflow) boundary for the characterization permeameter was designed to minimize impedance to outflow from the soil specimen. The outflow boundary consists of a 12-mm-thick steel outflow support plate with a system of fluid collection grooves. These grooves are sloped slightly toward a 3-mm diameter water outflow hole, which is shown in Fig. 5(b). A piece of filter paper underlain by a No. 100 wire screen was used to retain soil particles. For the soils evaluated as part of this study (clays of low plasticity), no soil particles were observed in the outflow reservoir. An o-ring groove along the perimeter of the support plate prevents water from leaking around the edges of the plate. As the seal between the outflow support plate and the underlying outflow reservoir is air tight, an air release pipe is used to maintain zero air pressure in the outflow reservoir. Specifically, a 3-mm-diameter steel pipe was passed through a hole in the support platen. The pipe was bent into a channel in the support platen so that it would be flush with the level of the permeameter base and passed through the permeameter wall with an "o-ring" seal. Measurements of water pressure in the outflow reservoir during infiltration, discussed in Section 6, confirm that air can freely escape from the outflow reservoir during infiltration. Although Fig. 5(a) shows two outflow transducers connected to the outflow reservoir, one has been replaced with a ball valve to collect water from the outflow reservoir after it is filled to capacity.

By imposing an infiltration rate and minimizing impedance to outflow, the boundary conditions in the centrifuge permeameter aim at reaching "open-flow" conditions (Conca and Wright 1992). In this case, the ψ in the soil specimen is not imposed at any point, as is done in SWRC testing in the UFA and SSC centrifuge approaches. Under open-flow conditions, it is possible that soil near the outflow face of the specimen will reach high degrees of saturation during steady-state water flow. This is because water will not flow out of an unsaturated soil until the pore-water pressure exceeds the pore air pressure (assumed to be atmospheric) at which point the water menisci become convex. The instrumentation in the centrifuge permeameter permits evaluation of the influence of open-flow boundary conditions on the ψ profile.

Data Acquisition and Instrumentation for Monitoring of Flow Variables in Unsaturated Soils

The centrifuge is equipped with a solid-state data acquisition board (no moving disk drives). The data acquisition system includes 32 analog input channels for various voltage-based transducers, with on-board amplification, filtering, and digitization. It also has 32 channels of digital input and output and 2 channels of video input for charged-coupled device cameras. Information is passed from the data acquisition system to an external computer as a digital TCP-IP signal over an ethernet cable with a fiber-optic rotary joint to transition from the spinning to stationary environments. Because transmission of data from the spinning environment is digital, electric noise from the induction motor of the centrifuge is not added to the data. The centrifuge has also a 24-channel slip ring stack for transmission of power and auxiliary data acquisition components [e.g., the RS232 cable for the time domain reflectometry (TDR) cable tester]. One important component of the centrifuge data acquisition system is the g meter, which is a load cell mounted to the test environment at a radial

location of 0.5 m. The self-weight deflection of the load cell during centrifugation was calibrated to the g level corresponding to midheight of the specimen. This permits continuous monitoring of the g level during centrifugation.

The instrumentation plan, shown in the cross section of the characterization permeameter in Fig. 5(b), was designed to minimize inclusions into the soil specimen. Inclusions may cause disturbance of the soil structure during insertion, affect the settlement pattern of the soil during centrifugation, and contribute to an increase in tortuosity, all of which may alter measurement of the K. Accordingly, rather than placing sensors within the soil specimen, the instrumentations for θ and ψ were embedded within the wall of the permeameter. The instrumentation in the centrifuge permeameter allowed nondestructive measurements of multiple variables, including outflow, average θ, and ψ in the specimen.

The volume of outflow from the soil specimen was inferred by measuring the water pressure at the base of the outflow reservoir. Specifically, a Druck PMP-4010 pressure transducer was connected to the outflow reservoir using a manometer tube. The sensing diaphragm of the transducer is at the same level as the base of the outflow reservoir. The transducer has a relatively low capacity (40 kPa) but can resolve small changes in pressure ($\sim$0.007 kPa). The measured water pressure at the base of the reservoir depends on both the g level and the height of water over the manometer tube. A minimum water volume of 10 mL is maintained in the outflow reservoir to provide a reaction against the self-weight deflection of the sensing diaphragm of the vertically oriented pressure transducer under the centripetal acceleration. However, the height of water in the reservoir does not necessarily indicate the volume of water in the outflow reservoir as nonuniformity in the g field may cause the surface of the water accumulated in the outflow reservoir to adopt a curved shape.

Because of the aforementioned considerations, the outflow transducers could not be calibrated using conventional calibration procedures outside of the centrifuge. Instead, calibration was performed by placing known volumes of water in the reservoir and spinning the permeameters to reach different g levels. Linear trends between the outflow volume and the transducer output voltage were obtained for different angular velocities, as shown in Fig. 6(a). The outflow transducer results shown in Fig. 6(b) are from a test on a permeameter without a soil specimen, in which the g level was varied in stages (as reflected by the changes in g level measured using the g meter) while maintaining a constant infiltration rate. As expected, the pressure transducer shows a linearly increasing output during steady-state flow. Also, the pressure transducer shows abrupt jumps when the g-level changes.

TDR was used in this study to infer changes in θ of the soil within the permeameter (Topp et al. 1980). This approach involves measuring the time required for an electromagnetic pulse to travel through a steel waveguide embedded within a soil layer. Due to the high dielectric permittivity of water (approximately 81) compared to that of soil particles (4) and air (1), the travel time of this pulse is particularly sensitive to the soil-water content (Jones et al. 2002). A single TDR waveguide was embedded longitudinally within the acrylic wall of the characterization permeameter, as shown in Fig. 5(b). The walls of the permeameter were shaped to hold the waveguide firmly in place while still exposing 70% of waveguide's surface area to the soil. As the TDR waveguide is held within a cavity in the waveguide wall, acrylic was selected as the permeameter material to minimize electrical interference. The vertical arrangement of the TDR waveguide was selected to accommodate space constraints and to avoid inclu-
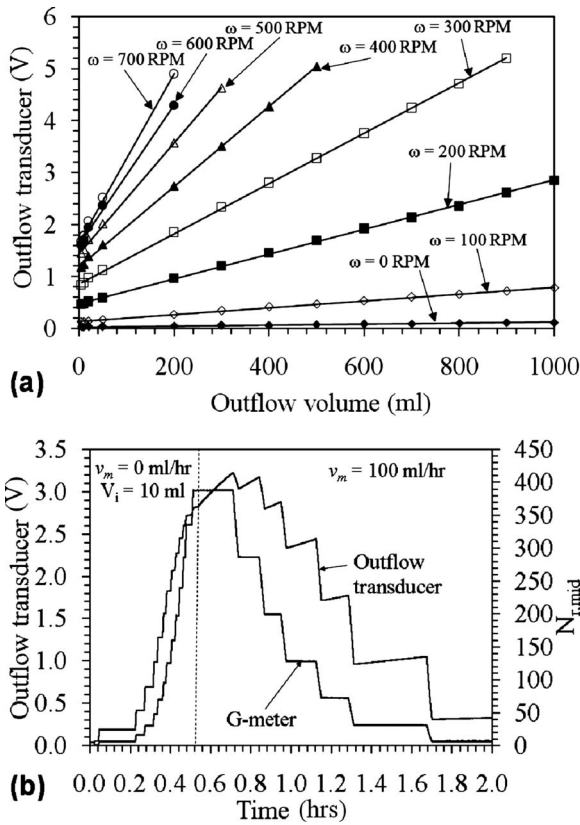
Fig. 6. (a) Outflow transducer calibration results; (b) outflow transducer and g meter results from an infiltration test under different g levels

Fig. 7. Calibration curve for TDR waveguide embedded in the characterization permeameter

sions into the soil specimen. This arrangement provides the average θ of the soil that is in direct contact with the length of the TDR waveguide. However, as will be discussed in the next section, the θ in the upper portion of the specimen is relatively constant during steady-state water flow. Accordingly, the average θ measured by the TDR in this orientation is suitable for measurement of the soil hydraulic characteristics under steady-state flow.

The TDR measurements were found not to be influenced by the increased centripetal acceleration or by the electrical field from the centrifuge motor (McCartney and Zornberg 2005). A soil-specific calibration curve of θ versus dielectric permittivity K_a was developed for a clay of low plasticity. The procedure involved bringing compacted clay specimen with the same dry density to steady-state flow conditions under different infiltration rates. The centrifuge was then stopped, a value of K_a of the soil was measured using the TDR, and a sample was obtained for gravimetric water content measurement. The calibration curve obtained using this procedure is shown in Fig. 7. The relationship between θ and dielectric permittivity is linear over the range of water contents observed during infiltration testing. The slope of the calibration curve is steeper (10.2%) than that for the waveguide buried in soil (11.8%). This reduction in slope is due to acrylic's relatively low dielectric permittivity of 3.4 (Jefferies and Koulouris 2003). However, because only 30% of the waveguide area is in contact with the acrylic, there is only a slight reduction in TDR sensitivity due to the partial embedment of the waveguide in the acrylic. The TDR measurement for an empty permeameter compared to the slope of the calibration curve with soils suggests that there may be some nonlinearity at low water contents (lower than those evaluated in the calibration testing program) due to the
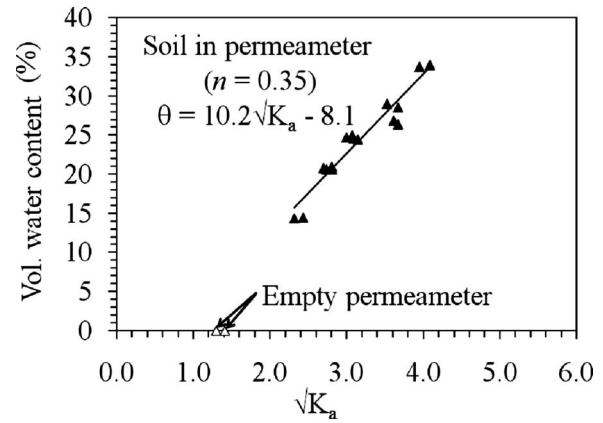
partial embedment of the waveguide. However, water contents in this range are not expected for infiltration testing in the centrifuge permeameter.

Three tensiometers were used to measure the distribution in ψ along the specimen height, as shown in Fig. 5(b). Tensiometers consist of a pressure sensor in a deaired water reservoir connected to a water-saturated, high-air-entry, porous ceramic stone embedded within a soil mass. In order to maintain continuity of ψ at the interface between the soil and the ceramic, water flows across the interface until the water pressure within the reservoir equals that in the soil (negative or positive). A schematic of the tensiometer designed for the characterization permeameter is shown in Fig. 8(a). This tensiometer has a brass housing that forms a 1-mL water reservoir between the sensing face of a vented Entran EPX-V01 pressure transducer (having a range of $\pm$ 700 kPa) and a porous ceramic cup set within a threaded brass pipe. The threaded brass pipe permits the porous stone to be boiled outside of the tensiometer, as well as interchanging of stones with different air-entry suction values. The porous ceramic cup having an air-entry value of 300 kPa incorporates a hollow cavity. This cavity was filled with a tightly wound filter paper. This approach was found to maintain a high K needed for rapid response while decreasing the "free" volume of water in the reservoir needed to measure values of ψ over 80 kPa without cavitation. The water reservoir of the tensiometer has a continuous flushing channel that allows removal of air bubbles during initial saturation and in case of cavitation. Before each test, the tensiometer was cycled between a positive pressure of 200 kPa and a negative pressure of 50 kPa.

The tensiometers could not be threaded directly into the acrylic of the permeameter without risking stress concentrations during centrifugation. Accordingly, an "o" ring was used around the circumference of the tensiometer to provide a hydraulic seal with a hole in the permeameter sidewall [see Fig. 5(b)]. The weight of the tensiometer was supported by a support bracket, shown in Fig. 5(c). The length of the tensiometer was selected so that the porous stone would intrude into the specimen by approximately 5 mm, ensuring intimate contact with the soil.

To evaluate the maximum ψ that can be measured, the tensiometer was placed in contact with a specimen of unsaturated clay which had been compacted dry of optimum. The ψ measurements obtained during this test are shown in Fig. 8(b). The tensiometer required less than 1 h to equilibrate with the ψ in the soil, but cavitation occurred shortly after reaching a ψ of 200 kPa. The flushing ports were then opened, and deaired water was injected
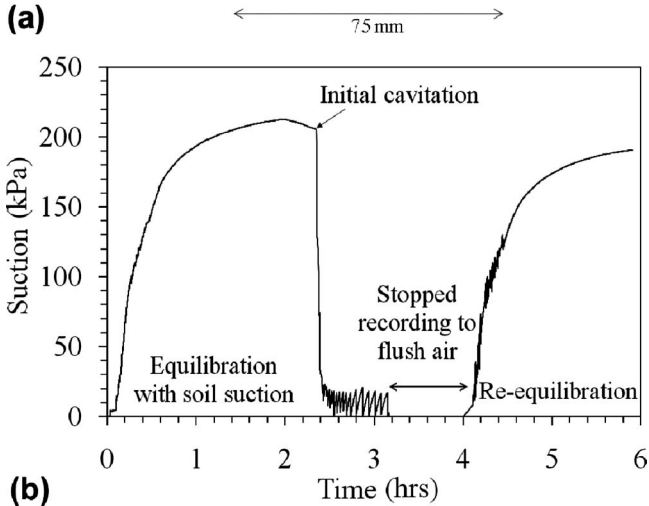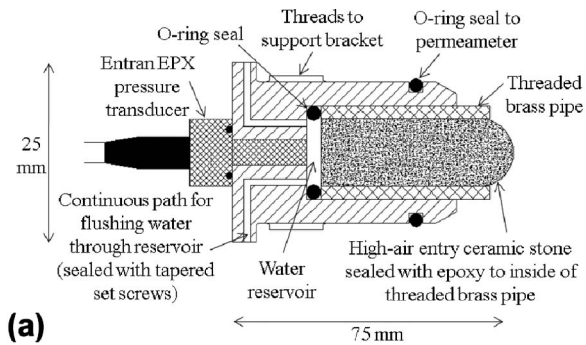
Fig. 8. Flushing tensiometer: (a) schematic view; (b) tensiometer cavitation test results

into one of the ports using a hypodermic needle. After flushing, the ports were closed and the tensiometer showed a similar equilibration response to that observed before cavitation. Although it is expected that the tensiometer may reach a higher capacity if prepressurization procedures were followed (Take and Bolton 2003), a ψ of 200 kPa was acceptable for the infiltration testing conducted as part of this study.

During an infiltration test, the tensiometer can measure transient changes in ψ, although transient responses are likely affected by the equilibration time of the tensiometer (approximately 30 min for large changes in ψ). However, as this study focuses on steady-state infiltration, the equilibration time is not a major issue. The measurements of the tensiometer are expected to be independent of the g level as the pressure diaphragm of the tensiometer is placed perpendicularly to the g field. Abrupt changes in the g level were observed to cause temporary changes in the ψ measurements, as changes in the weight of water within the tensiometer result in changes in measured water pressure. Nonetheless, this increase in water pressure within the tensiometer causes water to flow from the tensiometer, so the measured water pressure reequilibrates with the value of ψ in the soil.

Analysis of Data from the Centrifuge Permeameter

Several alternatives are possible for interpretation of the results from the permeameter, including steady-state infiltration analysis (Moore 1939), transient infiltration analyses such as the instantaneous profile method (Olson and Daniel 1981), or inverse analyses. The approach adopted in this study involves the use of steady-state infiltration analysis, which relies on interpretation of

the responses of the instrumentation after reaching equilibrium with an imposed flow condition on the soil specimen. Richards' equation for one-dimensional flow of water through unsaturated soil in a centrifuge permeameter is defined as

$$\frac{d\theta}{d\psi}\frac{\partial\psi}{\partial t} = \frac{\partial}{\partial z_m}\left[K(\psi)\left(\frac{\omega^2}{g}(r_0 - z_m) - \frac{1}{\rho_w g}\frac{\partial\psi}{\partial z_m}\right)\right] \quad (6)$$

This equation has been solved numerically by Šimůnek and Nimmo (2005). Numerical solution of Richards' equation for transient water flow in the centrifuge is particularly difficult as the slope of the SWRC ($d\theta/d\psi$) and the K function $K(\psi)$ are highly nonlinear. Further, the equation contains a quadratic term in the primary variable ψ (after expansion of the second term on the right hand side using the chain and product rules). However, Dell'Avanzi et al. (2004) developed an analytical solution to Richards' equation for steady-state water flow. Their solution involves the use of an exponential model to represent the K function (Gardner 1958) as follows:

$$K(\psi) = K_s e^{-\alpha\psi} \quad (7)$$

where α=fitting parameter and K_s=hydraulic conductivity of saturated soil. The ψ profile can be obtained as follows:

$$\psi(z_m) = -\frac{1}{\alpha}\ln\left[e^{[\ln|(v_m/N_rK_s)+e^{-\alpha\psi_0}|-\alpha\omega^2\rho_w z_m(r_0-z_m/2)]} - \frac{v_m}{N_rK_s}\right]$$

$$\text{if } (v_m/N_rK_s) + e^{-\alpha\psi_0} > 0$$

$$\psi(z_m) = -\frac{1}{\alpha}\ln\left[-e^{[\ln|(v_m/N_rK_s)+e^{-\alpha\psi_0}|-\alpha\omega^2\rho_w z_m(r_0-z_m/2)]} - \frac{v_m}{N_rK_s}\right]$$

$$\text{if } (v_m/N_rK_s) + e^{-\alpha\psi_0} < 0 \quad (8)$$

where ψ_0=suction at the outflow face of the centrifuge specimen. It should be noted that the N_r terms in Eq. (8) are a function of z_m [see Eq. (1)]. Although it is not necessary for characterization purposes, it was assumed that the suction at the outflow face of the specimen ψ_0 equals zero in the analyses shown in this section.

A comparison between the ψ profiles expected during steady-state infiltration, calculated using Eq. (8), with those expected at equilibrium (i.e., the case of no infiltration), calculated using Eq. (5), is shown in Fig. 9(a). The ψ profiles were calculated for an imposed surface discharge velocity, a saturated bottom boundary, and a soil layer characterized by values of $\alpha=0.2$ kPa^{-1} and K_s $=10^{-6}$ m/s (representative of a clay of low plasticity). The height to any point in the specimen z_m is normalized by the specimen height L_m. The equilibrium ψ profile increases linearly (a straight line if ψ was plotted on a natural scale). Both curves are identical near the base of the soil specimen, but the ψ profile during steady-state infiltration reaches a limiting value (referred to as ψ_∞) and remains relatively constant with height. The limiting ψ is sensitive to the soil type (i.e., to Gardner's α parameter), discharge velocity, and g level and can be calculated as follows:

$$\psi_\infty = -\frac{1}{\alpha}\ln\left(-\frac{v_m}{N_{r,mid}K_s}\right) \quad (9)$$

The limiting ψ is valid only when $N_r=N_{r,mid}$ throughout the profile. Otherwise, Eq. (8) can be used to predict ψ at a given height z_m. Because N_r varies with radius, the ψ distribution in the upper portion of the specimen shows a slight gradient. However, the ψ may be assumed constant in the upper portion of the specimen for the purpose of this analysis.

The pattern of the ψ profile, which shows a zone of relative constant ψ (equal to the limiting ψ), was an important aspect of
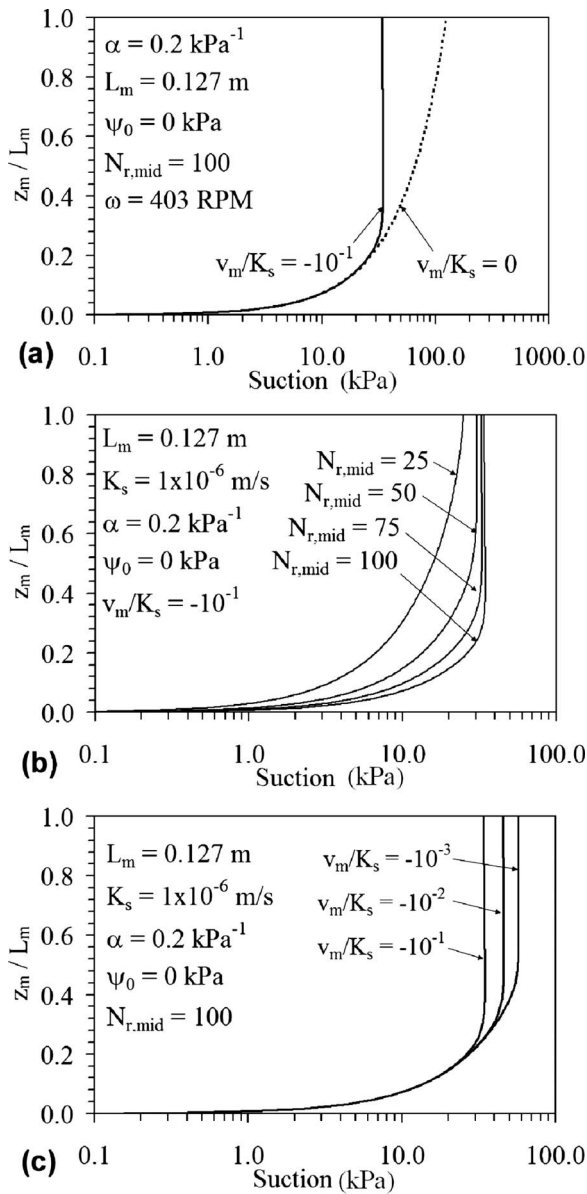
Fig. 9. Theoretical suction profiles in a centrifuge permeameter: (a) comparison between steady-state and equilibrium flow conditions; (b) steady state flow with different values of $N_{r,mid}$; and (c) steady state flow with different values of v_m

Fig. 10. Head profiles during steady-state infiltration in the centrifuge: (a) values; (b) gradients

the steady-state infiltration response under high g levels and was useful to design the instrumentation layout in the characterization permeameter. Specifically, the ψ profile during steady-state infiltration indicates that θ should also be relatively uniform in the upper zone of the specimen. Accordingly, the average θ inferred by the embedded TDR waveguide [Fig. 6(b)] is suitable to characterize the θ in the profile. Further, as the ψ is relatively constant in this zone, its gradient with z_m is negligible, which significantly simplifies Eq. (4). This observation was extended even further by Nimmo et al. (1987) and Conca and Wright (1992), who assumed that the ψ and θ profiles are constant throughout the entire soil specimen during steady-state infiltration in order to calculate the K using Eq. (4). Specifically, changes in θ were inferred via periodic measurements of the specimen weight outside of the centrifuge, which were assumed to be uniform in the soil specimen. It should be noted that an assumption of uniform ψ and θ is not

needed in this study. Also, the conditions leading to a uniform ψ profile may be assessed using in-flight measurements.

The effect of $N_{r,mid}$ on the ψ profile, while holding v_m constant, is shown in Fig. 9(b). The results in this figure indicate that the uniformity of the ψ profiles increases with increasing g level. That is, a greater length of soil in the upper portion of the specimen remains under constant ψ. The value of limiting ψ is also observed to be insensitive to the g level except for g levels below 25, where the ψ profile does not reach a limiting value within the height of the specimen. The effect of v_m on the ψ profile, while holding N_r constant, is shown in Fig. 9(c). The profiles in this figure indicate that the limiting ψ is sensitive to the discharge velocity. The length over which the ψ is uniform is similar for the three discharge velocities. Dell'Avanzi et al. (2004) observed that the ψ in the upper zone of the specimen, and specifically the limiting suction ψ_∞, is insensitive to the bottom boundary condition ψ_0.

A comparison between the magnitudes of the suction head profile, quantified for steady-state flow in the centrifuge using Eq. (8), the centrifuge elevation head profile, calculated using the first term on the left-hand side of Eq. (3), and the total head profile are shown in Fig. 10(a). The centrifuge elevation head is much larger in magnitude than the suction head. The influence of the suction head profile on the total head profile is only significant near the outflow boundary. The gradients of these head profiles are shown in Fig. 10(b). These results indicate that the total head gradient is dominated by the centrifuge elevation head gradient in the upper portion of the specimen, while it is controlled by the suction gradient near the bottom of the specimen.

The distribution of total head gradient with z_m during steady-state infiltration can be combined with Darcy's law [Eq. (4)] to estimate the distribution of K with z_m as follows:

(a)

(b)
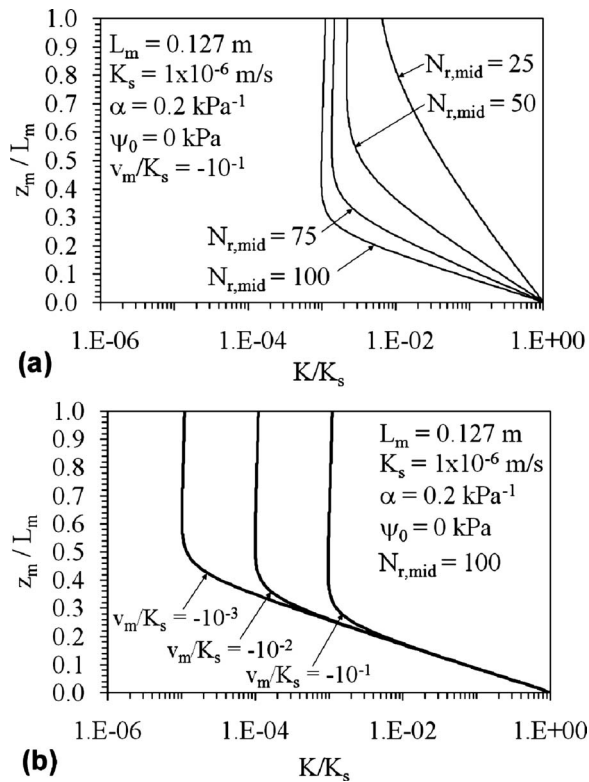
Fig. 11. Theoretical K profiles during steady-state infiltration in the centrifuge variation with: (a) $N_{r,mid}$; (b) v_m

$$K(\theta,\psi) = - \cfrac{v_m}{\cfrac{\omega^2}{g}(r_0 - z_m) - \cfrac{1}{\rho_w g}\cfrac{d\psi}{dz_m}} \qquad (10)$$

Distributions of K for different g levels are shown in Fig. 11(a) for the same conditions used in Fig. 11(b). The profiles of K shown in this figure indicate that the K can only be considered constant in the upper portion of the specimen for sufficiently high g levels. The g level above which K can be considered constant for the conditions shown in Fig. 11(a) is approximately 50 g's. It should be noted that the shape of the K profile is sensitive to the soil parameter α. Nonetheless, tensiometer measurements in the centrifuge permeameter would still permit characterization of a nonuniform K distribution. Distributions in K with varying discharge velocities are shown in Fig. 11(b) for the same conditions shown in Fig. 9(c). The K profiles shown in this figure indicate that changes in discharge velocity of one order of magnitude result in corresponding changes in K in the upper portion of the specimen of the same magnitude.

Geotechnical centrifuges are often used for scale modeling of earth structures. In this approach, any parameter that incorporates the coefficient of gravity (i.e., the unit weight of water or soil) must be scaled by $N_{r,mid}$ so that the behavior of the centrifuge model would be the same as a geometrically similar prototype that is $N_{r,mid}$ times larger. Some researchers have suggested that the hydraulic conductivity should be scaled. However, a conceptual example presented by Tan and Scott (1985) dispels this issue. Specifically, if a pressure gradient was applied to a soil specimen under zero gravity conditions, the hydraulic conductivity will still be equal to the coefficient of proportionality between the applied hydraulic gradient and the flow rate. The variation in hydraulic

conductivity with specimen height observed in Fig. 11(a) is due to the variation in hydraulic gradient with height in the specimen.

Typical Results from the Centrifuge Permeameter

The observations from theoretical analysis in the previous section justify the instrumentation plan of the centrifuge permeameter and permit interpretation of the monitoring results to define the soil hydraulic characteristics. Definition of a point on the SWRC and K function involves spinning a soil specimen under an infiltration rate Q (or discharge velocity $v_m = Q/A$) and angular velocity ω (or g level $N_{r,mid}$) until reaching steady state. At this point, not only the inflow rate but also the outflow rate, θ and ψ, remain constant with time. A simplified version of Eq. (10) can be used to estimate the magnitude of K in the upper portion of the soil specimen for the selected combination of v_m and ω imposed in the test. Specifically, this value of K, referred to as K_{target}, is defined by assuming that the suction gradient in Eq. (10) is negligible as follows:

$$K_{target} = - \left. \cfrac{v_m}{\cfrac{\omega^2}{g}(r_0 - z_m)} \right|_{z_m = 87 \ mm} \qquad (11)$$

The height of $z_m = 87$ mm is used in the definition of K_{target} as it corresponds to the height of the midpoint of the TDR waveguide. For the ranges of discharge velocities and angular velocities used in this study, K_{target} values range from 10^{-5} to 10^{-11} m/s. It should be noted that K_{target} is equal to the value of K defined using the SSC and UFA approaches.

The values of v_m, $N_{r,mid}$, and K_{target} for a typical test stage are shown in Fig. 12(a). Specifically, this stage is part of a test performed to define points on the SWRC and K function for a clay of low plasticity by maintaining the discharge velocity constant while changing the g level in stages. The full details of this test are discussed by McCartney and Zornberg (2010), in which the wetting and drying paths of the SWRC and K function are measured using different approaches. For this test stage, the imposed g level $N_{r,mid}$ was increased from 20 to 30 (see time $t=0$ in the figure) after reaching steady-state conditions in the previous test stage, while the discharge velocity was 3.5×10^{-7} m/s (the same as that imposed in the previous stage). The change in $N_{r,mid}$ resulted in a decrease in K_{target} from 1.8×10^{-8} to 1.2×10^{-8} m/s at the beginning of the stage. Accordingly, a decrease in θ and an increase in ψ with time are expected in the specimen as testing progresses.

The inflow and outflow volumes with time during this test stage are shown in Fig. 12(b). The outflow volume was obtained by applying the calibration equation at a g level of 30 g's to the outflow transducer voltage readings. At the beginning of the test stage, the outflow rate (i.e., the slope of the outflow volume versus time curve) was higher than the inflow rate, which remained constant throughout the test stage. However, after approximately 2 h the outflow and inflow rates reached the same value of 5 mL/h (corresponding to 3.5×10^{-7} m/s), which indicates that steady-state flow conditions were achieved in the specimen. The time-series measurements from the TDR waveguide and from the three tensiometers during centrifugation are shown in Fig. 12(c). The TDR data show a gradual decrease in θ from 30.5 to 28.7% and indicate that steady-state conditions were observed after about 3–4 h. The data from the three tensiometers indicate that the ψ throughout the specimen showed gradual increases in magnitude
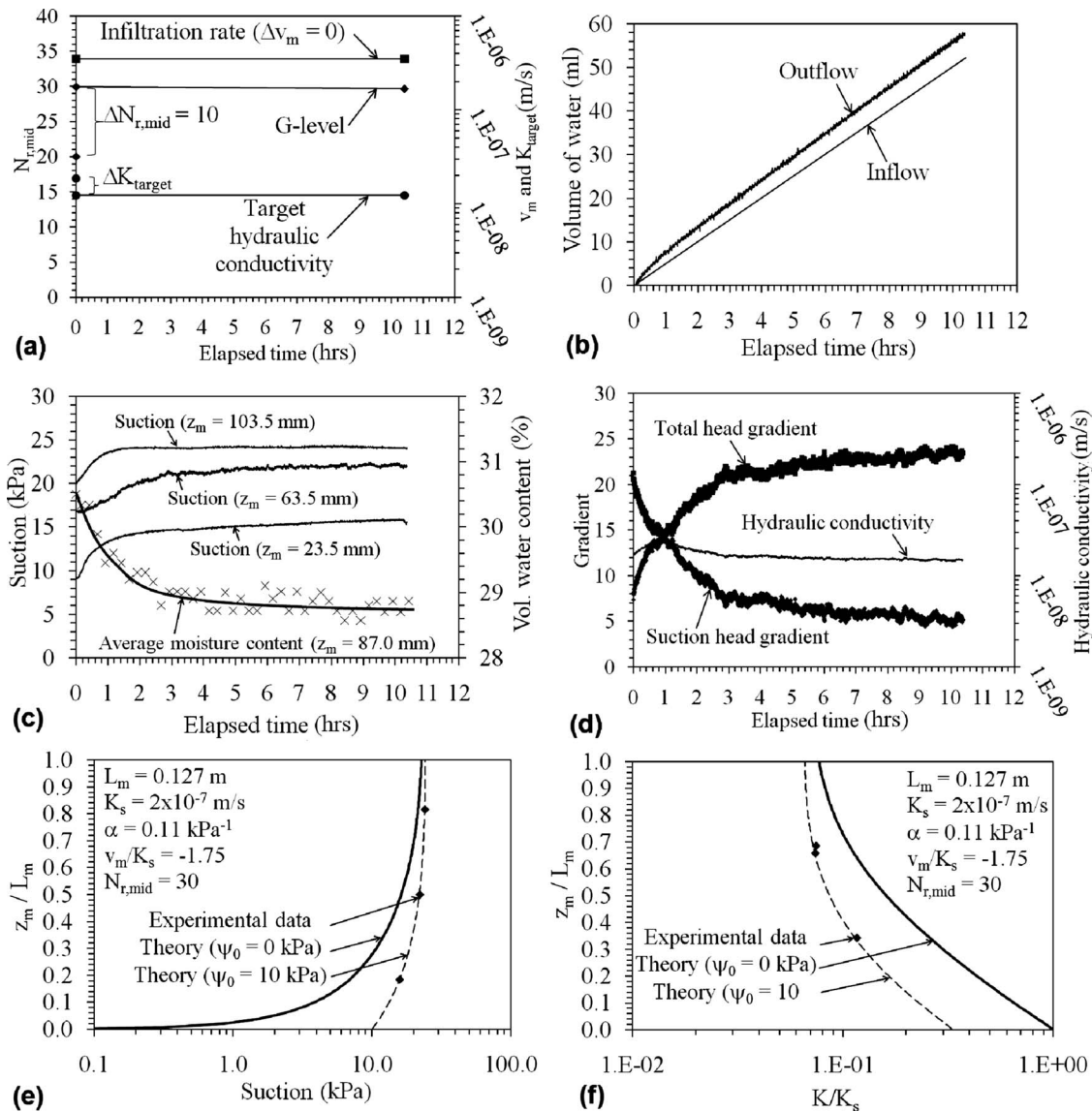
Fig. 12. Results from a centrifuge permeameter in a typical test stage: (a) target K value and control variables ($N_{r,mid}$ increased from 20 to 30 with a constant $v_m = 3.5 \times 10^{-7}$ m/s); (b) inflow and outflow; (c) suction and volumetric water content measurements; (d) calculated gradient and hydraulic conductivity; (e) theoretical and experimental suction profiles at steady state; and (f) theoretical and experimental hydraulic conductivity profiles at steady state

before stabilizing at constant values. The ψ at midheight of the TDR waveguide was interpolated from the ψ values measured by the tensiometers at heights of 103.5 and 63.5 mm and showed an increase in magnitude from 18.7 to 23.2 kPa. At steady state the ψ values measured by the two upper tensiometers are within 2 kPa of each other, which indicates that the ψ along the TDR waveguide is relatively constant. Accordingly, the average θ in the upper 80 mm of the specimen inferred by the TDR waveguide at steady state (28.7%) can be correlated directly with the ψ value calculated at the midheight of the TDR (23.2 kPa) to define a point on the SWRC. Although measurements of the θ and ψ during transient flow can also be correlated to define the SWRC, the θ during transient flow may not be uniform along the TDR waveguide, and the tensiometer may not have equilibrated with the ψ in the soil.

The ψ measurements from the tensiometers can be used to directly measure the suction gradient in Eq. (10). The gradients in suction head and total head during the test stage, calculated be-tween the heights of the upper two tensiometers, are shown in Fig. 12(d). These results indicate that the suction head gradient in the upper portion of the specimen was initially higher than the total head gradient but decreased from a magnitude of 21 to approximately 5 at steady state. As the centrifuge elevation head gradient is constant throughout the test (equal to the value of N_r = 28.5 g's at $z_m = 87$ mm), the total head gradient increases from 9 to a steady value of 25 during the stage. The value of K at an elevation of $z_m = 87$ mm was calculated from the total head gradient and discharge velocity using Eq. (10) and was also shown in Fig. 12(d). The measured K is approximately 1.5×10^{-8} m/s, which is slightly higher than the value of K_{target} estimated for this test stage.

The consistency of the measurements during this test stage with the results of the analytical solution developed in the previous section was evaluated. The measured ψ values at steady-state conditions with height along with the theoretical ψ profiles are shown in Fig. 12(e). The theoretical ψ profiles were defined by

selecting a value of $\alpha = 0.11$ kPa^{-1} in order to match the ψ value at $z_m = 103.5$ mm. In addition, different values of the ψ at the outflow face ψ_0 were selected to compare the influence of the outflow boundary condition. The ψ at the outflow face did not influence the ψ in the upper portion of the specimen significantly. A ψ of 10 kPa at the outflow face was found to provide a good match to the ψ values measured at the elevations of the tensiometers. In addition, the values of K defined using the total head gradients at three elevations (midheight of the TDR, midpoint between the upper and middle tensiometers, and midpoint between the middle and lower tensiometers) are compared with the theoretical predictions for this particular value of α in Fig. 12(f). The measured K values match the trend expected from the theoretical analysis for an assumed $\psi_0 = 10$ kPa. The results in Fig. 12(f) indicate that it may be necessary to consider the actual value of the suction head gradient in Eq. (10) rather than consider it negligible throughout the specimen as assumed in centrifuge permeameter approaches (Nimmo et al. 1987; Conca and Wright 1992). The data acquisition capabilities of the centrifuge permeameter help extend the range of ω and v_m that can be used for hydraulic characterization. This is especially the case for infiltration under low g levels, where K may not be uniform [see Fig. 11(a)].

It is interesting to note that, although the specimen height used in this analysis is relatively small ($L_m = 0.127$ m), the ψ profiles during steady-state infiltration are similar to those observed during steady-state infiltration through a 1.35-m soil profile performed in a 1-g setting (McCartney and Zornberg 2007). Centrifugation is therefore a useful tool to obtain the similar ψ profiles to those observed during infiltration through a relatively long soil column in a 1-g environment. Scaling of suction profiles in the centrifuge is discussed in more detail by Dell'Avanzi et al. (2004).

Conclusions

A new centrifuge permeameter was developed with the specific objective of expediting the measurement of the SWRC and K function of unsaturated soils. The centrifuge permeameter addresses concerns in the measurement of the hydraulic characteristics of unsaturated soils, including the time required to establish steady conditions. Specifically, experimental components were developed for infiltration control and nondestructive and continuous measurement of the outflow rate, θ, and ψ in flight during steady-state infiltration. Analytical solutions to Richards' equation for unsaturated water flow in the centrifuge were used to define the instrumentation layout and to assist in the interpretation of results from the instrumentation. The specific conclusions that can be drawn from this study include the following:

- A new centrifuge permeameter was developed, which allows in-flight monitoring of variables needed for direct measurement of the SWRC and K function of soils.
- Solutions to Richards' equation in the centrifuge indicate that a zone of uniform ψ, θ, and K develops in the upper portion of a soil specimen during steady-state infiltration in a centrifuge acceleration field. This validates the assumptions involved in the use of the UFA centrifuge method to determine the K function (ASTM D6527).
- Analytic solutions indicate that the limiting value to the ψ profile is sensitive primarily to the infiltration rate, while the length of soil over which the ψ is uniform is sensitive primarily to the g level. Although the ψ at the outflow boundary of

the specimen impacts the ψ distribution near the bottom of the specimen, the outflow boundary condition does not affect the ψ at the top of the specimen during steady-state infiltration. These theoretical observations were confirmed with measured values of outflow, ψ, and θ obtained in a typical test stage conducted to define a point on the SWRC and K function.
- The uniformity of the ψ profile in the upper portion of the specimen during steady-state infiltration under most g levels indicates that a vertically oriented TDR waveguide is suitable for measurement of the uniform θ that occurs in this portion of the specimen.

References

Arya, L. M., Leij, F. J., Shouse, P. J., and van Genuchten, M. (1999). "Relationship between the hydraulic conductivity function and the particle-size distribution." *Soil Sci. Soc. Am. J.*, 63, 1063–1070.

ASTM. (2000). "Standard test method for determining unsaturated and saturated hydraulic conductivity in porous media by steady-state centrifugation." *ASTM D6527*, American Society for Testing and Materials, West Conshohoken, Pa.

ASTM. (2002). "Standard test methods for determination of the soil-water characteristic curve for desorption using a hanging column, pressure extractor, chilled mirror hygrometer, and/or centrifuge." *ASTM D6836*, American Society for Testing and Materials, West Conshohocken, Pa.

Briggs, L. J., and McLane, J. W. (1907). "The moisture equivalent of soils." *U.S. Bur. Soils Bull.*, 45, 23.

Brooks, R., and Corey, A. (1964). "Hydraulic properties of porous medium." *Hydrology*, Colorado State Univ. Fort Collins. March, Paper No. 3.

Burger, C., and Shackelford, C. (2001). "Soil-water characteristic curves and dual porosity of sand-diatomaceous earth mixtures." *J. Geotech. Geoenviron. Eng.*, 127(9), 790–800.

Chiu, T.-F., and Shackelford, C. (1998). "Unsaturated hydraulic conductivity of compacted sand-kaolin mixtures." *J. Geotech. Geoenviron. Eng.*, 124(2), 160–170.

Conca, J., and Wright, J. (1992). "Diffusion and flow in gravel, soil, and whole rock." *Applied Hydrogeology*, 1, 5–24.

Dell'Avanzi, E., Zornberg, J. G., and Cabral, A. (2004). "Suction profiles and scale factors for unsaturated flow under increased gravitational field." *Soils Found.*, 44(3), 1–11.

Fredlund, D., and Rahardjo, H. (1995). *Soil mechanics for unsaturated soils*, Wiley, New York.

Gardner, R. (1937). "The method of measuring the capillary pressures in small core samples." *Soil Sci.*, 43, 277–283.

Gardner, W. (1958). "Some steady-state solutions of the unsaturated moisture flow equation with applications to evaporation from a water table." *Soil Sci.*, 85, 228–232.

Huang, S., Fredlund, D., and Barbour, S. (1998). "Measurement of the coefficient of permeability for a deformable unsaturated soil using a triaxial permeameter." *Can. Geotech. J.*, 35, 426–432.

International Society for Soil Mechanics and Foundation Engineering (ISSMGE). (1998). "Geotechnical centrifuge centers." *A Report Compiled by the Japanese Geotechnical Society*.

Jefferies, D. J., and Koulouris, A. (2003). "Dielectric loading of ADR antennas: Experimental results." *AntenneX*, 69, 7.

Jones, S. B., Wraith, J. M., and Or, D. (2002). "Time domain reflectometry measurement principles and applications." *Hydrolog. Process.*, 16, 141–153.

Khaleel, R., Relyea, J., and Conca, J. (1995). "Evaluation of van Genuchten–Mualem relationships to estimate unsaturated hydraulic conductivity at low water contents." *Water Resour. Res.*, 31(11), 2659–2668.

Lu, N., and Likos, W. (2005). *Unsaturated soil mechanics*, Wiley, New York.

McCartney, J. S. (2007). "Determination of the hydraulic characteristics of unsaturated soils using a centrifuge permeameter." Ph.D. thesis, The Univ. of Texas at Austin.

McCartney, J. S., and Zornberg, J. G. (2005). "The centrifuge permeameter for unsaturated soils." *Experus 2005*, A. Tarantino, E. Romero, and Y. J. Cui, eds., Balkema, Rotterdam.

McCartney, J. S., and Zornberg, J. G. (2007). "Effect of wet-dry cycles on capillary break formation in geosynthetic drainage layers." *Geosynthetics 2007*, IFAI, Washington, D.C.

McCartney, J. S., Zornberg, J. G., and Villar, L. (2007). "Estimation of the hydraulic conductivity function of unsaturated clays using an infiltration column test." *Proc., 4th Brazilian Conf. on Unsaturated Soils (NSAT)*, UFBA, Salvador, Brazil, 10.

Meerdink, J., Benson, C., and Khire, M. (1996). "Unsaturated hydraulic conductivity of two compacted barrier soils." *J. Geotech. Geoenviron. Eng.*, 122(7), 565–576.

Miller, C., Yesiller, N., Yaldo, K., and Merayyan, S. (2002). "Impact of soil type and compaction conditions on soil water characteristic." *J. Geotech. Geoenviron. Eng.*, 128(9), 733–742.

Moore, R. (1939). "Water conduction from shallow water tables." *Hilgardia*, 12, 383–426.

Ng, C., and Pang, Y. (2000). "Influence of stress state on soil-water characteristics and slope stability." *J. Geotech. Geoenviron. Eng.*, 126(2), 157–166.

Nimmo, J. (1990). "Experimental testing of transient unsaturated flow theory at low water content in a centrifugal field." *Water Resour. Res.*, 26, 1951–1960.

Nimmo, J., Rubin, J., and Hammermeister, D. (1987). "Unsaturated flow in a centrifugal field: Measurement of hydraulic conductivity and testing of Darcy's law." *Water Resour. Res.*, 23(1), 124–134.

Olson, R., and Daniel, D. (1981). "Measurement of the hydraulic conductivity of fine grained soils." *Permeability and groundwater contaminant transport (ASTM STP 746)*, T. F. Zimmie and C. O. Riggs, eds., ASTM, West Conshohoken, Pa., 18–47.

Parent, S.-E., Cabral, A., and Zornberg, J. G. (2007). "Water retention curve and hydraulic conductivity function of highly compressible materials." *Can. Geotech. J.*, 44(10), 1200–1214.

Puppala, A., Punthutaecha, K., and Vanapalli, S. (2006). "Soil water characteristic curves of stabilized expansive soils." *J. Geotech. Geoenviron. Eng.*, 132(6), 736–751.

Simms, P., and Yanful, E. (2002). "Predicting soil-water characteristic curves of compacted plastic soils from measured pore-size distributions." *Geotechnique*, 52(4), 269–278.

Šimůnek, J., and Nimmo, J. (2005). "Estimating soil hydraulic parameters from transient flow experiments in a centrifuge using parameter optimization technique." *Water Resour. Res.*, 41(4), 1–9.

Take, W. A., and Bolton, M. (2003). "Tensiometer saturation and the reliable measurement of matric suction." *Geotechnique*, 53(2), 159–172.

Tan, C. S., and Scott, R. F. (1985). "Centrifuge scaling considerations for fluid-particle systems." *Geotechnique*, 35(4), 461–470.

Tinjum, J., Benson, C., and Blotz, L. (1997). "Soil-water characteristic curves for compacted clays." *J. Geotech. Geoenviron. Eng.*, 123(11), 1060–1069.

Topp, G., and Miller, E. (1966). "Hysteretic moisture characteristics and hydraulic conductivities for glass-bead media." *Soil Sci. Soc. Am. Proc.*, 30, 156–162.

Topp, G. C., Davis, J., and Annan, A. (1980). "Electromagnetic determination of soil water content: Measurement in coaxial transmission lines." *Water Resour. Res.*, 16, 574–582.

van Genuchten, M. (1980). "A closed-form equation for predicting the hydraulic conductivity of unsaturated soils." *Soil Sci. Soc. Am. J.*, 44, 892–898.

Vanapalli, S., Pufahl, D., and Fredlund, D. (1999). "The influence of soil structure and stress history on the soil-water characteristic of a compacted till." *Geotechnique*, 49(2), 143–159.

Villar, L. F. (2002). "Study of the densification and desiccation of residual mineral waste from the processing of Bauxite." Ph.D. thesis, PUC-Rio, Brazil, 511.

Zapata, C., Houston, W., Houston, S., and Walsh, K. (1999). "Soil-water characteristic curve variability." *Advances in Unsaturated Geotechnics, Proc. of Sessions of Geo-Denver 2000, GSP No. 99*, ASCE, Denver.

Zornberg, J. G., LaFountain, L., and Caldwell, J. C. (2003). "Analysis and design of evapotranspirative cover for hazardous waste landfill." *J. Geotech. Geoenviron. Eng.*, 129(5), 427–438.

Zornberg, J. G., and McCartney, J. S. (2010). "Centrifuge permeameter for unsaturated soils II: Measurement of the hydraulic characteristics of an unsaturated clay." *J. Geotech. Geoenviron. Eng.*, 136(8), 1064–1076.